The Relationship between Ligand Aggregation and G-Quadruplex DNA Selectivity in a Series of 3,4,9,10-Perylenetetracarboxylic Acid Diimides†

Jonathan T. Kern, Pei Wang Thomas, and Sean M. Kerwin*

Division of Medicinal Chemistry and Institute for Cellular and Molecular Biology, College of Pharmacy, The University of Texas at Austin, Austin, Texas 78712

Received June 17, 2002; Revised Manuscript Received July 13, 2002

ABSTRACT: Human telomeres are comprised of d(TTAGGG) repeats that are capable of forming G-quadruplex DNA structures. Ligands that bind to and stabilize these G-quadruplex DNA structures are potential inhibitors of the cancer cell-associated enzyme telomerase. Other potential biological uses of G-quadruplex targeting ligands have been proposed. One particularly challenging aspect of the contemplated uses of G-quadruplex targeting ligands is their selectivity for G-quadruplex DNA versus double-stranded DNA structures. We have previously reported the observation that two structurally related 3,4,9,10-perylenetetracarboxylic acid diimide-based G-quadruplex DNA ligands, PIPER [*N*,*N*′-bis(2-(1-piperidino)-ethyl)-3,4,9,10-perylenetetracarboxylic acid diimide] and Tel01 [*N*,*N*′-bis(3-(4-morpholino)propyl)-3,4,9,10-perylenetetracarboxylic acid diimide], have different levels of G-quadruplex DNA binding selectivity at pH 7 as determined by absorbance changes in the presence of different DNA structures [Kerwin, S. M., Chen, G., Kern, J. T., and Thomas, P. W. (2002) *Bioorg. Med. Chem. Lett. 12*, 447−450]. Here we report that the less G-quadruplex DNA selective ligand PIPER can unwind double-stranded, closed circular plasmid DNA, as determined by a topoisomerase I assay. A model for the interaction of Tel01 with the G-quadruplex DNA structure formed by d(TAGGGTTA) was determined from NMR experiments. This model is similar to the previously published model for PIPER bound to the same G-quadruplex DNA and failed to provide a structural basis for the observed increased selectivity of Tel01 interaction with G-quadruplex DNA. In contrast, investigation into the aggregation state of Tel01 and PIPER as well as other 3,4,9,10-perylenetetracarboxylic acid diimide analogues bearing basic side chains demonstrates that ligand aggregation is correlated with G-quadruplex DNA binding selectivity. For all six analogues examined, those ligands that were aggregated at pH 7 in 70 mM potassium phosphate, 100 mM KCl, 1 mM EDTA buffer also demonstrated G-quadruplex DNA binding selectivity under these buffer conditions. Ligands that were not aggregated under these conditions display much lower levels of G-quadruplex DNA selectivity. The aggregation state of these ligands is extremely sensitive to the buffer pH. Tel01, which is aggregated at pH 7, is not aggregated at pH 6.4, where it demonstrates only modest G-quadruplex DNA binding selectivity, and PIPER in pH 8.5 buffer is both aggregated and highly G-quadruplex DNA-selective. To our knowledge, these studies demonstrate the first DNA structure selectivity as achieved through pH-mediated ligand aggregation. The potential impact of these findings on the selectivity of other classes of G-quadruplex DNA ligands is discussed.

Human telomeres are comprised of d(TTAGGG) repeats (*1*) and their associated telomere binding proteins. These terminal structures serve to protect the chromosomes from end-to-end fusion events and nuclease degradation, as well as acting to preserve essential genes throughout successive rounds of nuclear replication (reviewed in *2*). The extreme terminus of the telomere consists of a single-stranded DNA overhang of approximately 150 bases and serves as the primer for the enzyme telomerase (*3, 4*). Telomerase is a ribonucleoprotein expressed by 85−90% of all immortalized and cancer cells (*5*). Cells that express telomerase are capable of maintaining telomeric length throughout cellular replication, effectively ending cellular senescence and rendering the cells immortal (*6*).

Up to four guanosine-rich sequences, like those found in the single-stranded DNA overhang of the telomere, have been shown to associate to form unique secondary structures called G-quadruplexes. G-quadruplexes are comprised of stacked G-tetrads, in which four guanosines hydrogen-bond to form a planar, symmetrical ring that is capable of metal chelation (*7, 8*). When four separate G-rich DNA strands contribute to the G-quadruplex, it is an interstrand G-quadruplex (G4-DNA). If the four guanosines derive from the same DNA strand, then the G-quadruplex is referred to as an intrastrand G-quadruplex (G4′-DNA). Other G-quadruplex structures are also known to exist, but are beyond the scope of this work (reviewed in *9, 10*). G-quadruplex secondary structures negatively regulate telomerase activity, presumably by interfering with the ability of telomerase to load onto the

† This work was supported by grants from the Robert Welch Foundation (F-1298) and the National Institutes of Health (CA-67760).

* To whom correspondence should be addressed. E-mail: skerwin@mail.utexas.edu; Tel: (512)-471-5074.

10.1021/bi0263107 CCC: $22.00
Published on Web 08/29/2002

telomere (*11, 12*). Consequently, inhibition of telomerase through the stabilization of telomeric G-quadruplex DNA has become a focus of study in recent years (reviewed in *13*).

Several small molecules have been identified that interact with G-quadruplex DNA (*14*−*25*). Some of these compounds have also demonstrated telomerase inhibition (*20*−*23, 26*−*28*). G-quadruplex interactive ligands are generally polycyclic, aromatic ligands substituted at multiple positions. Unfortunately, the selectivity for G-quadruplex DNA over double-stranded DNA of these compounds is often less than ideal, resulting in nonspecific cellular cytotoxicity (*10, 18, 19, 29*−*33*). Increased selectivity for G-quadruplex DNA over double-stranded DNA and the corresponding decrease in cytotoxicity is an essential goal for these G-quadruplex ligands and their use as telomerase inhibitors, or as biological probes for in vivo detection of G-quadruplex. It is therefore necessary to examine the mechanism of observed selectivity for G-quadruplex interactive ligands in order to rationally design ligands with improved G-quadruplex selectivity.

Using the DOCK shape-complementarity scoring algorithm (*34*), we have previously identified the 3,4,9,10-perylenetetracarboxylic acid diimides (PTCDIs)[1] as potential G-quadruplex interactive molecular scaffolds (*35*). The *N*,*N*′-bis(2-(1-piperidino)ethyl)-3,4,9,10-perylenetetracarboxylic acid diimide (PIPER) was shown to interact with intermolecular G-quadruplex DNA (G4-DNA) through aromatic stacking interactions with available 3′ or 5′ G-tetrad faces of a $[d(GGG)]_4$ core. The stabilization of G-quadruplex DNA by PIPER may be responsible for its observed telomerase inhibition. Once bound to G-quadruplex DNA, PIPER has been demonstrated to disrupt the unwinding of the quadruplex by yeast *Sgs*I helicase, a member of the RecQ DNA helicase family closely related to human Bloom's syndrome helicase and human Werner's syndrome helicase (*36*). PIPER also facilitates the formation of G-quadruplex DNA from single-strand DNA (*37*) as well as certain duplex oligonucleotides (*38*). In ^{1}H NMR experiments, however, there is no evidence for PIPER binding to duplex DNA (*35, 38*). The perylene diimide *N*,*N*′-bis(3-(dimethylamino)propyl)-3,4,9,10-perylenetetracarboxylic acid diimide, DAPER, is known to precipitate trace amounts of calf thymus DNA, providing evidence for double-stranded DNA binding (*39*). Like porphyrins (*40*), these planar, heterocyclic aromatic PTCDIs are known to self-assemble through stacking interactions (*41*). This aggregate formation may occur at a nucleation site as in the case of ligands aggregating on DNA templates, which has been previously reported (*42*−*44*). Alternatively, these ligands may aggregate separately from the DNA in solution, resulting in an aggregate capable of binding DNA or sequestering ligand from ligand−DNA interactions.

In a brief communication, we have recently reported our initial studies on the G-quadruplex selectivity of PIPER and *N*,*N*′-bis(3-(4-morpholino)propyl)-3,4,9,10-perylenetetracarboxylic acid diimide (Tel01) (*14*). We observed that Tel01 was much more selective for G-quadruplex DNA over double-stranded DNA than PIPER in pH 7 potassium phosphate buffer, conditions which favored the aggregation of Tel01 but not PIPER. We concluded that PIPER and Tel01 bind preferentially to G-quadruplex DNA under conditions that favor ligand aggregation. Here we expand on our previous findings, utilizing a series of PTCDIs with various sidearm groups and studying the structural basis of G-quadruplex interaction, double-stranded DNA interaction, aggregation state, and G-quadruplex selectivity. By comparing NMR-based models of PIPER and Tel01 bound to G-quadruplex DNA, we find that there is no structural basis for the difference in G-quadruplex selectivity between these PTCDIs. Rather, the aggregation state of these molecules is critical to their G-quadruplex selectivity. This ligand aggregation is pH-dependent and related to the pK_a of the various PTCDI sidearm nitrogen substituents. We show that this pH-dependent aggregation mediates the relative G-quadruplex binding selectivity of a range of PTCDI ligands. Also, we provide evidence for the intercalation of monomeric PTCDIs into double-stranded DNA. The discovery of a unique mechanism of binding selectivity based on ligand aggregation expands our knowledge of the PTCDI class of compounds and may have implication for other G-quadruplex DNA ligands.

Scheme 1: Synthesis of 3,4,9,10-Perylenetetracarboxylic Acid Diimides (PTCDIs)

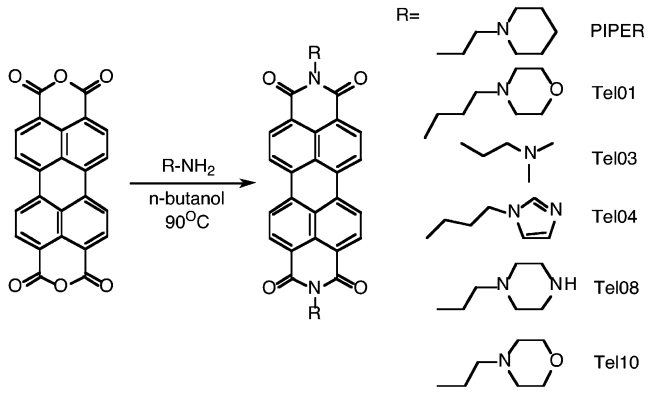

MATERIALS AND METHODS

Sample Preparations. PIPER was prepared as previously reported (*35*). Tel01, Tel03, Tel04, Tel08, and Tel10 (Scheme 1) were prepared from 3,4,9,10-perylenetetracarboxylic acid dianhydride (100 mg, Aldrich) by reaction with the appropriate primary amine (10 equiv) in 20 mL of 1-butanol at 90 °C for 24 h with stirring under an argon atmosphere. The reaction mixture was cooled to room temperature, and the product was isolated by filtration, washed with deionized water and methanol, and dried under vacuum. Compounds were characterized by ^{1}H and ^{13}C NMR spectroscopy and low and high-resolution chemical ionization mass spectroscopy. (a) *N*,*N*′-Bis(3-(4-morpholino)propyl)-3,4,9,10-perylenetetracarboxylic acid diimide (Tel01) 91% yield. ^{1}H NMR (CF_3COOD, 300 MHz, 25 °C) δ: 8.68 (s, 8H), 4.45−4.54 (m, 8H), 4.19 (s, 4H), 3.84 (s, 4H), 3.46−3.59 (m, 8H), 2.53 (s, 4H); ^{13}C NMR (CF_3COOD, 300 MHz, 25 °C) δ: 167.65, 137.75, 134.80, 131.03, 127.96, 126.28, 123.66, 66.05, 57.86, 54.63, 39.64, 24.29. CIMS *m*/*z* 645 (MH^+). HRCIMS calcd for $C_{38}H_{37}N_4O_6$ 645.27131; found, 645.27223. (b) *N*,*N*′-Bis-(2-(dimethylamino)ethyl)-3,4,9,10-perylenetetracarboxylic acid

[1] Abbreviations: BSA, bovine serum albumin; EDTA, *N*,*N*,*N*′,*N*′-ethylenediaminetetraacetic acid; EtBr, ethidium bromide; PTCDI, 3,4,9,10-perylenetetracarboxylic acid diimide; RLS, resonance light scattering; TFA, trifluoroacetic acid; SDS, sodium dodecyl sulfate; Tris, *N*,*N*,*N*-tris(hydroxymethyl)aminomethane.

diimide (Tel03) 89% yield (*45*). ^{1}H NMR (CF_3COOD, 300 MHz, 25 °C) δ: 8.88 (d, J = 7.9, 4H), 8.80 (d, J = 7.9, 4H), 4.79 (s, 4H), 7.77 (s, 4H), 3.21 (s, 12H); ^{13}C NMR (CF_3COOD, 300 MHz, 25 °C) δ: 168.58, 138.75, 135.51, 131.63, 128.72, 126.78, 123.75, 60.54, 46.23, 46.19. CIMS *m*/*z* 533 (MH^+). HRCIMS calcd for $C_{32}H_{29}N_4O_4$ 533.21888; found, 533.22029. (c) *N*,*N*′-Bis(3-(1-imidazolyl)propyl)-3,4,9,10-perylenetetracarboxylic acid diimide (Tel04) 93% yield. ^{1}H NMR (CF_3COOD, 500 MHz, 50 °C) δ: 9.28 (s, 2H), 9.21 (s, 8H), 8.06 (s, 2H), 7.97 (s, 2H), 5.01 (s, 4H), 4.95 (s, 4H), 3.06 (s, 4H); ^{13}C NMR (CF_3COOD, 500 MHz, 25 °C) δ: 168.21, 138.46, 137.21, 135.58, 131.74, 128.70, 126.90, 124.61, 124.37, 122.77, 50.37, 40.43, 30.83. CIMS *m*/*z* 607 (MH^+). HRCIMS calcd for $C_{36}H_{27}N_6O_4$ 607.20937; found, 607.20801. (d) *N*,*N*′-Bis(2-(1-piperazinyl)ethyl)-3,4,9,10-perylenetetracarboxylic acid diimide (Tel08) 91% yield. ^{1}H NMR (CF_3COOD, 500 MHz, 50 °C) δ: 9.41 (d, J = 7.9, 4H), 9.35 (d, J = 7.9, 4H), 5.40 (s, 4H), 5.02 (br, 4H), 4.57 (s, 12H), 4.44 (br, 4H); ^{13}C NMR (CF_3COOD, 500 MHz, 25 °C) δ: 168.63, 138.94, 135.74, 131.79, 128.93, 126.87, 123.82, 59.35, 51.95, 44.22, 37.59. CIMS *m*/*z* 615 (MH^+). HRCIMS calcd for $C_{36}H_{35}N_6O_4$ 615.27198; found, 615.27273. (e) *N*,*N*′-Bis(2-(4-morpholino)ethyl)-3,4,9,10-perylenetetracarboxylic acid diimide (Tel10) 95% yield. ^{1}H NMR (CF_3COOD, 500 MHz, 50 °C) δ: 9.35 (d, J = 7.18, 4H), 9.31 (d, J = 7.63, 4H), 5.33 (s, 4H) 4.85 (d, J = 6.40 Hz, 4H), 4.60 (t, J = 10.53 Hz, 4H), 4.50 (t, J = 3.24 Hz, 4H), 4.34 (s, 4H), 3.94 (br, 4H); ^{13}C NMR (CF_3COOD, 500 MHz, 25 °C) δ: 168.57, 138.89, 135.72, 131.75, 128.87, 126.88, 123.88, 66.38, 59.48, 55.52, 37.59. CIMS *m*/*z* 617 (MH^+). HRCIMS calcd for $C_{36}H_{33}N_4O_6$ 617.24001; found, 617.23944.

DNA Preparation. The four oligonucleotides d(TAGGGTTA), d(TTAGGG)$_4$, d(CGCGCGATATCGCGCG), and d(TTTTTTTT) were synthesized on a 10 μM scale using a PerSeptive Biosystems Expedite 8909 automatic DNA synthesizer and columns from Glen Research. Oligos were cleaved from the columns and HPLC-purified on a C-18 column. Collected fractions were combined and extensively dialyzed against deionized water before being lyophilized completely. DNAs were dissolved in 70 mM potassium phosphate/100 mM KCl/1 mM EDTA buffer at the appropriate concentration and pH for study. The G-quadruplex DNAs and the double-stranded DNA were heated to 90 °C for 5 min and slowly cooled to anneal the strands. DNA structures were confirmed using nondenaturing gel electrophoresis. Throughout this work, DNA concentrations are expressed in terms of DNA structure, which is the same as DNA strand concentration for single-stranded and intramolecular G-quadruplex DNA, half the DNA strand concentration for double-stranded DNA, and one-fourth the DNA strand concentration for four-stranded intermolecular G-quadruplex DNA.

NMR Spectroscopy. G-quadruplex DNA [d(TAGGGTTA)]$_4$ in 90% H_2O/10% D_2O with 150 mM KCl, 25 mM potassium phosphate, 1 mM EDTA (pH 7) was titrated with a solution of Tel01 in 0.1% aqueous TFA. Spectra were recorded at 27 °C utilizing a standard jump−return pulse sequence for water suppression (*46*) with a relaxation delay of 2 s. Spectra of the 1:1 G4-DNA [d(TAGGGTTA)]$_4$−Tel01 complex in D_2O with 150 mM KCl, 25 mM potassium phosphate, 1 mM EDTA (pH 7) were recorded at 40 °C utilizing a 500 MHz Varian Unity plus NMR. Mixing times of 100, 200, and 300 ms were used. Based upon NOE build-up curves (data not shown), the 200 ms mixing time was chosen for cross-peak intensity analysis. All of the nonexchangeable DNA protons, excluding the 5′ and 5″ sugar protons, were readily assigned following sequential assignment procedures (*47*). The agreement between the assigned 2′ and 2″ protons in both the COSY and NOESY confirms accurate assignments of the DNA protons. The aromatic protons of Tel01 were assigned based on their strong COSY correlation. Assignments of the proton resonances for the Tel01 sidearm could be made following the methylene protons of the alkyl linker via both NOESY and COSY.

Modeling and Refinement. Using Macromodel 6.5 (Schrodinger, Inc.) and the previously published [d(TAGGGTTA)]$_4$ G-quadruplex as the beginning DNA model, Tel01 was built and manually positioned within the G-quadruplex to best satisfy the NOE interactions between the aromatic protons of Tel01 and the G5 C1′ protons and T6 C1′ protons of the quadruplex as observed in the 200 ms NOESY spectra. The complex was transferred to the INSIGHT II suite of programs (Molecular Simulations, Inc.) for restraint analysis and refinement using the CFF91 force field. Distance restraints (144 DNA to DNA restraints, 14 Tel01 to DNA restraints) were input as calculated from the 200 ms NOESY experiment and classified as strong (2.0−2.9 Å), medium (2.5−4.0 Å), or weak (3.5−5.0 Å) following the reasoning outlined for our previously published model (*35*). The Tel01 complex was subjected to restrained molecular dynamics (50 ps at 250 K), sampling 15 structures for conjugate gradient minimization to an energy convergence of 0.001 kcal/mol.

Facilitation of G-quadruplex Formation. DNA, d(TAGGGTTA), in water was heated to 90 °C for 5 min before being rapidly cooled in ice to ensure that the DNA was all single-stranded. This DNA stock solution (8 μL) and various concentrations of PTCDI in water (2 μL) were combined with 10 μL of 140 mM potassium phosphate buffer (pH 7) containing 200 mM KCl and 2 mM EDTA. The reaction mixtures were allowed to incubate at room temperature for 1 or 16 h. Following incubation, 4 μL of loading buffer (0.25% bromophenol blue, 0.25% xylene cyanol, 40% glycerol) was added, and the samples were electrophoresed on a 1.5 mm thick, 20% polyacrylamide native gel at 130 V with standard Tris−boric acid−EDTA (TBE) as running buffer. DNA was visualized by UV-shadowing, and the gel images were recorded by digital photography and quantified using NIH Image software.

Fluorescence Spectroscopy. Spectra were recorded on a Hitachi model F-2000 spectrofluorometer. For fluorescent scans, compound (1 μM) in 70 mM potassium phosphate/100 mM KCl buffer/1 mM EDTA at the cited pH was allowed to equilibrate for 1 h before scans were performed at 25 °C using an excitation wavelength of 520 nm and emission wavelengths from 530 to 800 nm. The quartz cuvette was treated with SigmaCote for 1 h followed by extensive washing with water to minimize nonspecific binding of the ligand to the cuvette. Resonance light scattering experiments were performed on the same samples by synchronizing the excitation and emission wavelengths and recording the emission intensity every 10 nm from 220 to 650 nm.

Absorption Spectroscopy. Spectra were recorded on a UNICO model 2102 UV spectrophotometer. To determine the best conditions under which to pursue the visible absorption studies with the perylene diimides, we first determined their propensity for nonspecific binding under the conditions of the absorption spectroscopy experiments. Each of three perylene diimide compounds (Tel01, Tel03, and PIPER) was dissolved in 70 mM potassium phosphate/100 mM KCl/1 mM EDTA buffer at 25 μM and stored for 10 min in polystyrene cuvettes at room temperature. The solutions were withdrawn, and the absorbance of the solutions was compared to that immediately before storage in the cuvettes. While solutions of Tel01 and Tel03 demonstrated negligible change in absorbance, solutions of PIPER demonstrated ~11% loss of absorbance due to nonspecific binding to the polystyrene cuvettes. A survey of other materials (glass, silanized glass, polypropylene, silanized polypropylene) indicated even more pronounced nonspecific binding of PIPER (24−33% loss in absorbance at 10 min) and significant nonspecific binding by Tel01 and Tel03 to glass and polypropylene at 10 min. Longer storage times generally led to increased nonspecific binding, so that after 1 h the absorption decrease for Tel03 solutions was 79% in glass vials, but only 3% in polystyrene cuvettes. Thus, all subsequent experiments were carried out in polystyrene cuvettes. For pH-dependent absorption spectra, compound (20 μM) was incubated at room temperature in 40 mM potassium phosphate buffer at the indicated pH. For DNA binding experiments, the absorption spectra were obtained for the compound (20 μM) in 70 mM potassium phosphate/100 mM KCl/1 mM EDTA buffer (pH 7) alone or in the presence of 20 μM structure of G4-DNA $[d(TAGGGTTA)]_4$, G4′-DNA $[d(TTAGGG)_4]$, double-stranded DNA $[d(CGCGCGATATCGCGCG)]_2$, or single-stranded DNA d(TTTTTTTT). Samples were monitored until equilibrium was achieved, as evidenced by constant absorbance readings.

Topoisomerase I Unwinding Assay. Topoisomerase I unwinding assays were performed following the procedure of Shen (*48*). Double-stranded phage ΦX174 DNA (Sigma) was used without purification. The supercoiled DNA was relaxed with calf thymus topoisomerase I (Amersham Pharmacia Biotech) per the manufacturers' recommendations in the supplied buffer. Relaxed ΦX174 DNA (250 ng) was dispensed in reaction buffer (50 mM Tris-HCl, pH 7.5, 20 mM KCl, 1 mM Na-EDTA, 1 mM DTT, 30 μg/mL BSA) to a final volume of 15 μL. A 20× drug stock solution (or reaction buffer for control) was added, and the drug/DNA mixture was incubated at 25 °C for 30 min. PIPER concentrations ranged from 5 to 200 μM. Ethidium bromide was used as a positive control at concentrations of 1 and 2.5 μM. Topoisomerase I (10 units, where 1 unit is the amount of enzyme needed to completely relax 0.5 μg of supercoiled pBR322 DNA in 20 μL in 30 min at 37 °C) was added and the mixture incubated at 37 °C for 90 min. Loading solution (2% SDS, 14% ficoll, 0.1% bromophenol blue in water) was added and the mixture subjected to electrophoresis (1% agarose gel in TBE, 20 V, 18 h). During this electrophoresis, the drug is removed from the DNA, as has been reported by Shen (*48*). The gel was stained with ethidium bromide, destained in deionized water, and visualized using a Chemi-Imager 4000 system (Alpha Innotech Corp.). Quantification of the visualized DNA bands was achieved using NIH Image software.

RESULTS

A variety of PTCDIs were prepared by reacting commercially available 3,4,9,10-perylenetetracarboxylic acid dianhydride with a variety of primary amines, present in excess in warm 1-butanol as solvent (Scheme 1). Isolation of pure PTCDIs was carried out by filtration of the reaction mixture followed by washing the crude product with water and methanol to remove the unreacted amine. The solid PTDCIs obtained after extensive drying in vacuo were characterized by ^{1}H and ^{13}C NMR and high-resolution chemical ionization mass spectrometry. The PTCDIs that were prepared included the previously reported *N*,*N*′-bis(piperidinoethyl) derivative PIPER and *N*,*N*′-bis(morpholinopropyl) derivative Tel01 as well as the *N*,*N*′-bis(dimethylaminoethyl) analogue Tel03, the *N*,*N*′-bis(imidazolylpropyl) analogue Tel04, the *N*,*N*′-bis(piperazinylethyl) analogue Tel08, and the *N*,*N*′-bis(morpholinoethyl) analogue Tel10.

The PTCDI Tel01 Binds $[d(TAGGGTTA)]_4$ by Stacking on the 3′ Terminal G-Tetrad. The structural basis of G-quadruplex DNA recognition by small molecules is still not well understood. One mode of interaction between planar chromophores and G-quadruplex DNA involves end-stacking of the chromophore on one or both available G-tetrad faces of a G-quadruplex. This binding mode has been observed for the PTCDI PIPER binding to the four-stranded G-quadruplex d(TAGGGTTA), as determined by solution NMR data (*35*). Martin and Neidle have also reported X-ray fiber diffraction data on the 1,4-disubstituted amidoanthraquinone BSU-1071's interaction with a synthetic $[d(TGGGGT)]_4$ sequence which also demonstrated this G-tetrad stacking motif (*18*). In contrast, solution NMR data for the interaction of distamycin with the intermolecular G-quadruplex $[d(TGGGGT)]_4$ have demonstrated the cooperative binding of two or more distamycin molecules to the grooves of the G-quadruplex (*49*). The information gleaned from these structural studies of G-quadruplex DNA and ligand complexes with G-quadruplex DNA aids greatly in rational drug design and helps to explain various differences in the observed binding of ligands to G-quadruplex DNA. Our preliminary absorption spectroscopy experiments indicated that PIPER and Tel01 have strikingly different selectivity for G-quadruplex DNA over double-stranded DNA at pH 7 (*14*). Here, we present a model of the Tel01−$[d(TAGGGTTA)]_4$ complex derived from NMR data for comparison with the previously published PIPER−$[d(TAGGGTTA)]_4$ complex model. The similarity of these two models indicates that the differing G-quadruplex selectivity of these two PTCDIs is not caused by different modes of binding between the ligands and the DNA.

The intermolecular G4-DNA $[d(TAGGGTTA)]_4$ has previously been shown to be a reasonable structure to investigate the binding of ligands, specifically PTCDIs (*25*, *35*). When this G-quadruplex structure is titrated with Tel01 in 90% H_2O/10% D_2O/175 mM potassium buffer, a pronounced upfield shift of the imino protons of the G-quadruplex DNA is observed as the ligand to DNA structure ratio approaches 1:1 (Figure 1A). With the addition of Tel01 beyond the 1:1

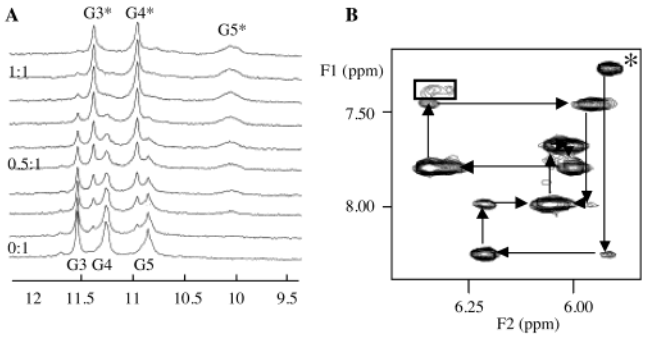

FIGURE 1: (A) NMR titration of G4-DNA $[d(TAGGGTTA)]_4$ with Tel01. The imino proton region of the 500 MHz spectra is shown at 27 °C. The G3, G4, and G5 labels indicate the imino protons of the G-quadruplex prior to Tel01 addition. With the introduction of Tel01, the imino proton resonances shift upfield until a 1:1 stoichiometry is achieved (G3*, G4*, and G5*). (B) The aromatic to C1′ proton region of the 2D NOESY spectra of the $[d(TAGGGTTA)]_4$−Tel01 complex recorded at 40 °C. The arrows follow the sequential proton assignments of the DNA while the box indicates the interactions between the G5* and T6* C1′ protons with the aromatic protons of Tel01.

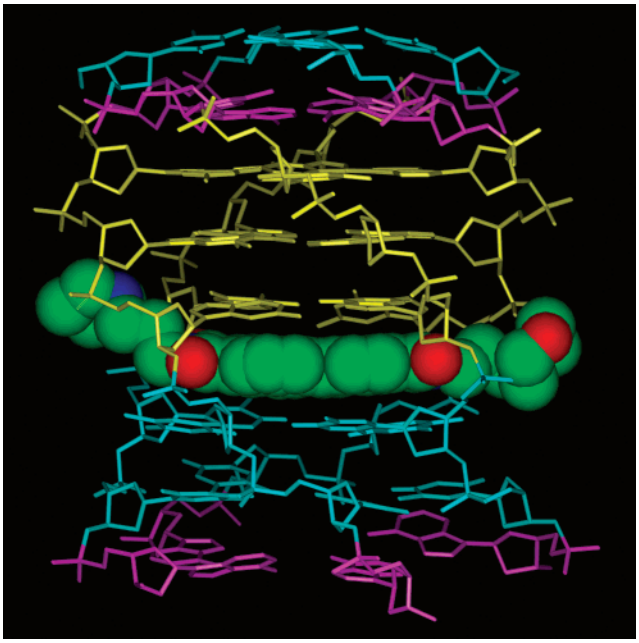

FIGURE 2: NMR-based model of the Tel01−$[d(TAGGGTTA)]_4$ complex. The ligand is stacked on the 3′ G-tetrad face with the morpholinopropyl sidearms positioned in the grooves of the DNA. The DNA thymine residues are shown in aqua, adenines in purple, and guanosines in yellow. The ligand is CPK-rendered with carbons in green, oxygen in red, and nitrogen in blue. Hydrogens are removed for clarity.

stoichiometry, we observe a third set of imino proton resonances (data not shown) indicative of a second lower-affinity binding site as seen with the PIPER−$[d(TAGGGTTA)]_4$ complex (*35*). Beginning at the 5′ end of the DNA sequence, we number the residues T1, A2, G3, G4, G5, T6, T7, and A8. In this titration experiment, the G5 imino proton's peak shifts the furthest, indicating that the ligand binds close to this position, the 3′ terminal face of the G-quadruplex DNA. Both the free DNA G3, G4, and G5 imino proton peaks and the G3*, G4*, and G5* imino proton peaks of the Tel01−$[d(TAGGGTTA)]_4$ complex are observed in the spectra at less than stoichiometric amounts of ligand. This indicates that the DNA−ligand complex is in slow-exchange with free DNA. Once the ligand−DNA complex is formed, however, only one set of DNA imino proton peaks is observed in the spectra. The absence of additional DNA imino proton peaks indicates that the complex maintains the C_4 symmetry of the free G-quadruplex. In order for C_4 symmetry to be retained in the complex, the ligand must transition between the two C_2-symmetrical binding configurations on the terminal G-quartet face. These 90° transitions are apparently fast on the NMR time scale.

Sequential walk assignments for the aromatic to C1′H portion of the 200 ms 2D-NOESY spectrum of the Tel01−$[d(TAGGGTTA)]_4$ complex are shown in Figure 1B. Beginning in the upper right quadrant of the figure with the cross-peak between the DNA's T1 C6H resonance and T1 C1′H resonance (* in Figure 1B), assignments of the aromatic to C1′ proton resonances of the complex are made by following the connectivity between the cross-peak resonances. Assignments of the C3′ and C4′ proton resonances are accomplished similarly, while assignment of the 2′ and 2″ proton resonances may be made by comparison with the aromatic region of the NOESY and confirmed in the COSY spectra. Cross-peaks between Tel01's aromatic protons and both the G5* C1′H and T6* C1′H of the G-quadruplex DNA are shown in the box in Figure 1B. These DNA−ligand cross-peaks indicate that the ligand aromatic protons interact with the G-quadruplex DNA at this base step. Unfortunately, the close proximity of the G5* C8H and the T6* C6H signals does not allow us to determine if there is the expected lack of connectivity between these two base steps in the sequential walk assignments. The NOESY and COSY data are satisfied by placing the ligand sandwiched between the 3′ terminal guanine tetrad and the subsequent thymine residues as shown in the NMR-derived model of the Tel01−$[d(TAGGGTTA)]_4$ complex (Figure 2). The alkyl linker protons of the Tel01 sidearms show weak NOE cross-peaks with the G5* C1′, T6* C1′, and G5* C3′ protons of the G-quadruplex. As these NOE cross-peak intensities are weak, and the symmetry of the quadruplex is maintained, we believe that the sidearms are dynamic and free to move throughout the groove, interacting with each of these DNA protons transitionally. These NOE requirements may be satisfied by a dynamic model with each sidearm contacting either the G5* C1′ and T6* C1′ protons or the G5* C3′ protons in two rapidly interconverting overall binding configurations of the G-quadruplex. The model shown is a representation of this dynamic model showing one morpholinopropyl sidearm in contact with the G5* C1′H/T6* C1′H and the other in contact with the G5* C3′H of the DNA.

As in our previous PIPER model, we note relatively weak NOE interactions between the two thymine residues and the adenine residues in the 3′ tail of the G-quadruplex. We expect that the tail region of the G-quadruplex is loosely stacked and offers little resistance to the previously mentioned fast 90° transition of the ligand on the 3′ terminal G-tetrad face.

We demonstrate here that there are no qualitative differences between the PIPER−$[d(TAGGGTTA)]_4$ complex and the Tel01−$[d(TAGGGTTA)]_4$ complex that could play a role in the difference in G-quadruplex selectivity for these compounds. We note the potential for the PTCDI arm substituents to be in dynamic movement throughout the G-quadruplex grooves, transitionally interacting with both sides of the groove. These data present evidence that PIPER

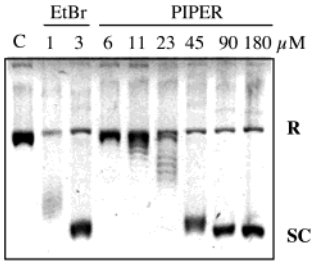

FIGURE 3: Topoisomerase I DNA unwinding assay results for PIPER and ethidium bromide (EtBr) as a positive control. Relaxed ΦX174 phage DNA in 50 mM Tris, 20 mM KCl, 1 mM EDTA, 1 mM DTT, 30 μg/mL BSA at pH 7.5 was incubated alone (lane C) or with either EtBr or PIPER at the concentrations shown at 25 °C for 30 min followed by the addition of calf thymus topoisomerase I (10 units) and further incubation at 37 °C for 90 min. The samples were treated with SDS (2%) and ficoll (14%) and the DNA topoisomers separated by electrophoreses (1% agarose, 20 V, 18 h) and visualized by EtBr staining. At concentrations above 6 μM PIPER, the relaxed DNA (R) is converted to supercoiled DNA (SC) as a result of ligand-induced DNA unwinding.

and Tel01, representative of this class of PTCDIs containing basic sidearm substituents, bind similarly to this parallel-stranded G-quadruplex and that observed differences in selectivity for this structure over double-stranded DNA might instead relate to the inherent physical properties of each specific PTCDI.

The PTCDI PIPER Binds to and Unwinds Double-Stranded DNA. While the binding of the perylene compounds to G-quadruplex DNAs has been studied with NMR, very little information has been provided for the interaction of this class of compounds with double-stranded DNA. Under appropriate conditions, the absorbance spectra of these PTCDI ligands undergo a pronounced bathochromic shift in the presence of double-stranded DNA (see below). Under these same conditions, the fluorescence spectrum of these ligands is quenched in the presence of double-stranded DNA (data not shown). To gain more insight into the nature of the double-stranded DNA binding observed for members of the PTCDI class, we turned to a DNA unwinding assay. Topoisomerase I unwinding assays have been used to demonstrate the interactions of elsamicin A and a number of quinobenzoxazines with plasmid DNA (*48*). Here, we demonstrate that PIPER in pH 7.5 reaction buffer demonstrates the DNA unwinding indicative of an intercalating ligand. During our initial experiments to determine the effective working concentration of PIPER, we noted that topoisomerase I relaxation of supercoiled ΦX174 phage DNA to relaxed closed circular DNA was inhibited at concentrations above 300 μM PIPER (data not shown). This inhibition is most likely due to extensive DNA binding at these high concentrations of ligand. In the absence of added compound (PIPER or EtBr), relaxed DNA incubated with topoisomerase I does not form supercoiled DNA; however, in the presence of 1 and 2.5 μM aliquots of the intercalator ethidium bromide, topoisomerase I converts relaxed DNA to supercoiled DNA (Figure 3). In the presence of increasing amounts of added PIPER, the relaxed ΦX174 phage DNA is converted to supercoiled DNA in a concentration-dependent manner. The minimum unwinding concentration (MUC) of PIPER is approximately 11 μM, and the PIPER concentration at which half of the DNA is converted to supercoiled DNA (UC_{50}) is 35 μM. As will be discussed later, other PTCDIs (such as Tel01) aggregate under the reaction conditions required for the experiment, so they could not be similarly assayed. The MUC and UC_{50} values for PIPER are similar to those reported for other intercalators, such as the quinobenzoxazines (*48, 50*).

PTCDIs Facilitate G-quadruplex Formation. Assembly, as opposed to stabilization, of G-quadruplex structures from suitable single-stranded or double-stranded DNA by small molecules may be linked to their in vivo mechanisms of action and perhaps play a role in telomerase inhibition. The ability to facilitate the formation of G-quadruplex DNA structures from single-stranded DNA has been reported for a variety of G-quadruplex interactive ligands, including ethidium derivatives (*23*), dibenzophenanthrolines (*27*), and the PTCDI PIPER (*37*). PIPER has also been shown to promote the formation of G-quadruplex DNA structures from certain double-stranded DNA sequences (*38*). To determine if this facilitation of G-quadruplex structures is unique to the PTCDI PIPER or whether it applies to other PTCDI molecules, we examined the ability of PIPER and Tel01 to facilitate the formation of four-stranded G-quadruplex DNA structure from the single-stranded DNA. This information could further assist in ruling out this ligand characteristic as a possible basis for our observed difference in G-quadruplex selectivity over double-stranded DNA between PIPER and Tel01. For these studies, we employed the same d(TAGGGTTA) oligonucleotide used in the NMR structural investigations described above. As this DNA sequence lacks the ability to form intramolecular DNA structures, the results of this facilitation study were not complicated by concentration-dependent effects on the distribution of four-stranded, two-stranded, and other G-quadruplex structures (*37*). Single-stranded d(TAGGGTTA) DNA was incubated alone or in the presence of PTCDIs at room temperature in 70 mM potassium phosphate buffer containing 100 mM KCl, 1 mM EDTA at pH 7, and the DNA products were separated by native polyacrylamide gel electrophoresis and visualized by UV shadowing. The results for Tel01, which are similar to those for PIPER, are shown in Figure 4A. In the absence of added PTCDI, there is very little G-quadruplex DNA formed; however, the formation of G-quadruplex is readily apparent in the presence of the ligand, and the amount of G-quadruplex increases with increasing ligand concentration. Similar results are obtained if the gel is visualized by staining with ethidium bromide, which binds to and stains G4-DNA (*52*); increasing concentration of PTDCIs resulted in increased intensity of the ethidium bromide stained G4-DNA band (data not shown). The PTCDIs PIPER and Tel01 behave similarly in this facilitation assay (Figure 4C). Both PTCDIs facilitate the formation of G4-DNA to approximately the same extent, indicating that the observed difference in G4-DNA binding selectivity between these two PCTDIs is not reflected in a difference in facilitation properties.

Advantageously, the PTCDIs are highly colored under normal lighting conditions. By comparing the gels under both UV and normal lighting conditions, we observe that the G-quadruplex DNA band, visible under UV light, comigrates with a visible red band of the PTCDI (Figure 4B). Because the uncomplexed PTCDIs do not migrate toward the anode, the observation of a PTCDI band that comigrates with the DNA suggests that the PTCDI remains bound to the G-quadruplex during electrophoresis, indicative of relatively

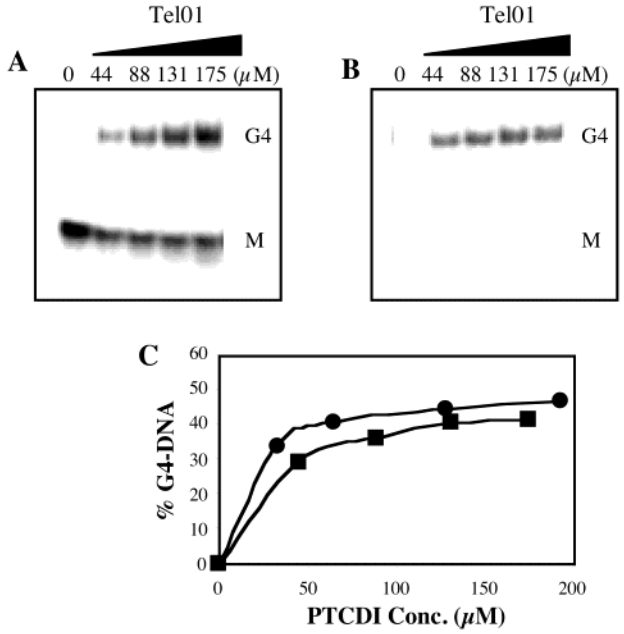

FIGURE 4: Facilitation of G-quadruplex DNA formation from single-stranded DNA d(TAGGGTTA) by PTCDIs. Single-stranded d(TAGGGTTA) in 70 mM potassium phosphate, 100 mM KCl, 1 mM EDTA (pH 7) was incubated with various concentrations of Tel01 or PIPER at room temperature, and the resulting DNA structures were separated by electrophoresis on a 20% polyacrylamide gel under native conditions. The DNA was visualized by UV shadowing. (A) Representative gel showing increased formation of G4-DNA (G4) from single-stranded DNA (M) with increasing concentration of Tel01 after 16 h incubation at room temperature. The gel was visualized by UV-shadowing. (B) Same gel as in (A) under visible light, demonstrating the migration of the red PTCDI with the G4-DNA band. (C) Graphical representation of the G4-DNA facilitation due to PIPER (circles) and Tel01 (squares) after 1 h incubation.

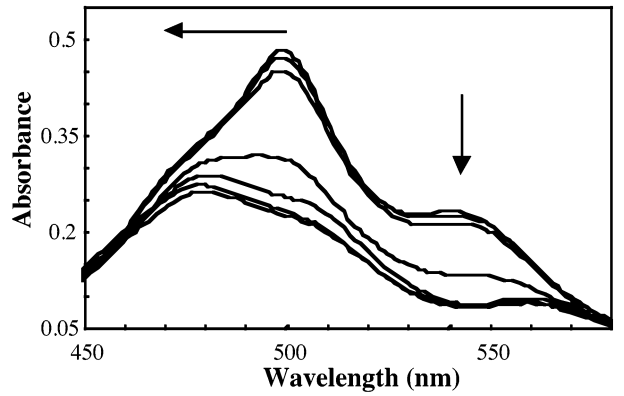

FIGURE 5: Absorption spectra of Tel01 in 40 mM potassium buffer at different pHs. The lines represent pH 1, 2, 4, 6, 7, 8, and 10, respectively, from top to bottom. With increasing pH, the absorption maximum is shifted from 500 to 480 nm while there is a decrease in absorbance at 550 nm. Tel01 aggregates between pH 6 and 7.

tight binding. This result also highlights the driver role (*37*) played by PTCDIs in G-quadruplex DNA facilitation; the G-quadruplex DNA structure, once formed, associates tightly with the PTCDI, providing a thermodynamic driving force for conversion of single-stranded DNA to G-quadruplex.

PTCDI Aggregation Is pH-Dependent. Visible absorbance spectroscopy analysis of the PTCDIs in varying pH buffers reveals interesting results (Figure 5). When 20 μM Tel01 is placed in 40 mM potassium phosphate buffer at pH from 1 to 10, the maxima absorption shifts from 500 to 480 nm. This shift is accompanied by a decrease in absorbance at 550 nm. This visible absorbance shift correlates to the aggregation of the PTCDI as evidenced by resonance light scattering (RLS) experiments. For aggregates in which there is good overlap between adjacent monomer chomophores, a large increase in the intensity of scattered light is observed when the incident light is the same wavelength as the aggregate absorbance (*52*). As shown in Figure 6, there is a strong RLS signal at 480 nm for solutions of Tel01 (1 μM) in 70 mM potassium phosphate buffer containing 100 mM KCl and 1 mM EDTA at pH values of 6.4 and higher. The pH-dependent RLS spectrum maximum at 480 nm corresponds with the pH-dependent visible absorbance shift to a wavelength maximum at 480 nm noted previously in Figure 5, indicative of a shift from nonaggregated Tel01 at pH below 6 to extensively aggregated compound at pHs above 6.4. The aggregation of Tel01 is extremely sensitive to small changes in pH; there is a particularly abrupt increase in the RLS signal for Tel01 solutions between pH 6.4 and 6.5 (Figure 6). At pH 7, the RLS signal decreases somewhat due either to precipitation of the aggregate or to a change in the nature of the aggregate. Further increase in the pH much above pH 7 results in precipitation of the compound. It should be noted that the aggregation phenomenon is expected to be dependent on conditions such as PTCDI concentration and solution ionic strength as well as pH. We have observed aggregation of solutions of Tel01 (20 μM) at pH 6, but only at high ionic strength (1 M NaCl). In contrast, even at concentrations as low as 1 μM in 40 mM potassium phosphate buffer at pH 7, Tel01 is extensively aggregated, as evidenced by RLS.

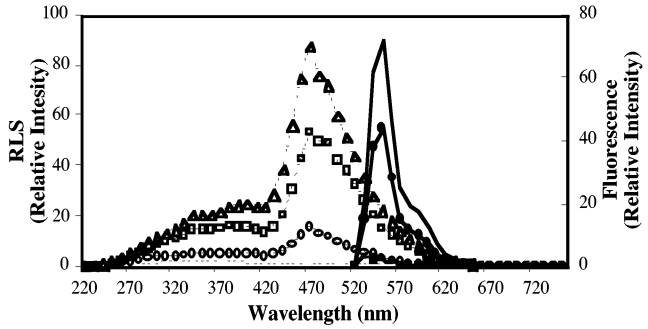

FIGURE 6: Resonance light scattering (dashed lines) and fluorescence spectra (solid lines) of 1 μM Tel01 in 70 mM potassium phosphate, 100 mM KCl, 1 mM EDTA buffer at pH 6 (no marker), 6.4 (circles), 6.5 (triangles), and 7 (squares). With increasing pH, the aggregation of Tel01 is marked by an increase in the RLS signal and a decrease in the fluorescence intensity.

Previous fluorescence studies of PTCDI self-association have demonstrated that self-association results in quenching of the PTCDI fluorescence (*53*), indicative of the formation of face-to-face association (H-aggregate) as opposed to a staggered arrangement (J-aggregate) (*54*). Because the fluorescence quantum yields of monomeric PTCDIs are very high (ca. 1) and relatively insensitive to the nature of the *N*-substitutents (*55*), the determination of the fluorescence intensity of solutions of these compounds provides a convenient method to monitor the degree of aggregation. The RLS profile of the PTCDIs can thus be used to monitor aggregate formation at various pHs while fluorescence spectroscopy can simultaneously be used to monitor the presence of monomeric ligand in solution. In Figure 6, the

Table 1: Relationship between PTCDI Aggregation and G-quadruplex Selectivity

PTCDI[b]	fluorescence[c]	ΔA_{550nm}[a] in presence of G4-DNA[d]	G4′-DNA[e]	dsDNA[f]	ssDNA[g]	relative G-quadruplex selectivity[h]
PIPER	207.8	0.45	0.76	0.23	0.11	2.0
Tel01	1.3	0.57	0.82	0.03	0.00	19.0
Tel03	285.7	0.61	nd[i]	0.44	0.12	1.4
Tel04	3.4	0.60	0.45	0.03	0.01	20.0
Tel08	18.2	0.87	0.49	0.27	0.03	3.2
Tel10	2.3	0.52	0.54	0.01	0.02	52.0
PIPER (pH 8.5)[j]	9.1	0.42	nd	0.01	nd	42.0
Tel01 (pH 6.4)[j]	141.1	0.65	nd	0.41	nd	1.6

[a] Difference between the A_{550nm} of a 20 μM solution of the PTCDI in 70 mM potassium phosphate, 100 mM KCl, 1 mM EDTA buffer, pH 7, in the presence of the DNA sample (20 μM structure) and in the absence of the DNA. [b] For structures, see Figure 1. [c] Relative fluorescence intensity (arbitrary units) of the 550 nm emission peak of the PTCDI (1 μM) in 70 mM potassium phosphate, 100 mM KCl buffer, pH 7 (excitation at 520 nm). [d] $[d(TAGGGTTA)]_4$. [e] $[d(TTAGGG)_4]$. [f] $[d(CGCGCGATATCGCGCG)_2]$. [g] d(TTTTTTTT). [h] Ratio of ΔA_{550nm} in the presence of G4-DNA to ΔA_{550nm} in the presence of dsDNA. [i] Not determined. [j] Experimental conditions are the same as in footnotes *a* and *c*, except the pH of the buffer was as noted.

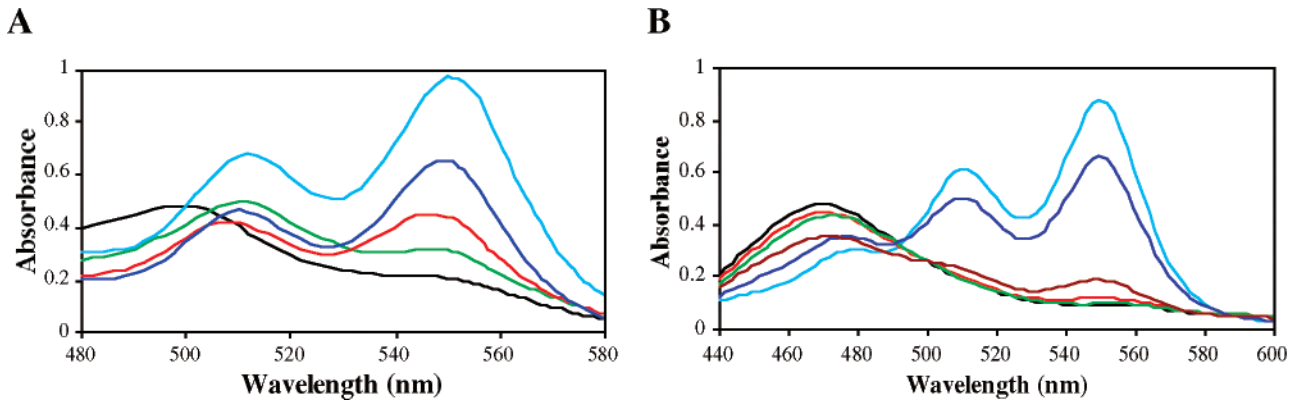

FIGURE 7: Absorption spectra of 20 μM PIPER (A) and Tel01 (B) alone (black) or with 20 μM (structure) of G4-DNA $[d(TAGGGTTA)]_4$ (blue), G4′-DNA $[d(TTAGGG)_4]$ (cyan), ssDNA d(TTTTTTTT) (green), or dsDNA $[d(CGCGCGATATCGCGCG)]_2$ (red), in 70 mM potassium phosphate, 100 mM KCl, 1 mM EDTA buffer at pH 7. The compounds and DNA structures were combined in a 1:1 stoichiometry, except for the curve in brown, in which the concentration of the dsDNA structure was 120 μM (1:96 drug/DNA base pair stoichiometry). Binding is apparent by monitoring the change in absorbance at 550 nm. Tel01 shows marked selectivity for the G-quadruplex DNAs over double- and single-stranded DNA when compared to PIPER under these conditions.

increase in the RLS emission signal of Tel01 as the pH is increased from 6 to 6.5 is accompanied by concomitant decrease in the fluorescence emission signal due to the monomeric ligand in solution (second *y*-axis, Figure 6).

The other PTCDIs shown in Scheme 1 also undergo pH-dependent aggregation as evidenced by absorption spectroscopy, RLS, and fluorescence; however, the pH at which aggregation occurs depends on the nature of the basic sidearms of the PTCDI. The absorption spectra of the other PTCDIs (20 μM) in various pH buffers show a pH-dependent shift from 500 nm at lower pH to 480 nm at higher pH, similar to that shown for Tel01 in Figure 5. The pH at which aggregate formation occurs for the various PTCDIs as determined by these absorbance changes is 7.5 for PIPER, 6.5 for Tel01, 7.5 for Tel03, and 5.5 for Tel04. Tel08 displays more complex pH-dependent spectral changes, with transitions noted at pH 6 and between pH 10 and 12. These results roughly correlate with the expected pK_a of the basic side chains of these PTCDIs; Tel04, with the least basic imidazole-containing side chain, undergoes aggregation at the lowest pH, while PIPER and Tel03, with the most basic side chains, undergo aggregation only at higher pH. At the physiologically relevant pH used in the DNA binding studies (pH 7), each PTCDI has a differing aggregation state. PIPER and Tel03 exist as monomeric species, whereas Tel01, Tel04, and Tel10 exist mainly as aggregate species. The fluorescence data in Table 1 for solutions of each PTCDI in pH 7 buffer provide further evidence for this phenomenon. At pH 7, solutions of both PIPER and Tel03 have high relative fluorescence intensities, due to a higher percent of non-aggregated PTCDI in solution. The other ligands have very low fluorescent intensities, indicating that at this pH they exist predominantly as aggregates in solution.

PTCDI Self-Association Is Correlated with G-quadruplex Binding Selectivity. The changes in the absorbance spectra of solutions of PTCDIs (20 μM) in pH 7.0 potassium phosphate buffer (170 mM K^+) alone or in the presence of 20 μM single-stranded DNA (ssDNA) [d(TTTTTTTT)], double-stranded DNA (dsDNA) [d(CGCGCGATATCGCGCG)]$_2$, intermolecular G-quadruplex DNA (G4-DNA) $[d(TAGGGTTA)]_4$, or intramolecular G-quadruplex DNA (G4′-DNA) $[d(TTAGGG)_4]$ were determined. Under these conditions, certain PTCDIs demonstrate a much more pronounced change in their absorbance spectrum in the presence of G-quadruplex DNA than in the presence of single- or double-stranded DNA. As exemplified by the spectra obtained for Tel01 (Figure 7B), the spectra of these PTCDIs change from the 480 nm peak indicative of aggregated ligand in the absence of G-quadruplex DNA to two longer wavelength absorbance peaks at 510 and 550 nm

in the presence of either G4-DNA or G4′-DNA. In contrast, in the presence of ssDNA, the spectra of these PTCDIs show only a slight decrease in the absorbance at 480 nm, and in the presence of dsDNA, this decrease at 480 nm is accompanied by a slight increase in the absorbance at 550 nm. Addition of a large excess of dsDNA (120 μM structure) results in only modest further change at 480 and 550 nm (Figure 7B). The PTCDIs that display this selective interaction with G-quadruplex DNA versus single- or double-stranded DNA are the PTCDIs that were found to be extensively aggregated at pH 7: Tel01, Tel04, and Tel10. In contrast to the results obtained with PTCDIs that are extensively aggregated at pH 7, the PTCDIs that are less aggregated at pH 7 demonstrate substantial changes in their absorbance spectra in the presence of ssDNA, dsDNA, and G-quadruplex DNA. These PTCDIs, exemplified by PIPER, undergo an absorbance spectral shift from 498 nm for the ligand alone to 510 nm in the presence of all the DNA samples (Figure 7A). In addition, in the presence of G4-DNA, G4′-DNA, and dsDNA, this shift is accompanied by the appearance of an intense new peak at 550 nm (Figure 7A). These nonselective PTCDIs include PIPER, Tel03, and Tel08.

Quantification of the binding selectivity of these PTCDIs is complicated by the aggregation of the ligands. Absorbance titrations of solutions of PTCDIs with various DNA samples under conditions in which the PTCDIs are aggregated do not lead to isosbestic behavior, and Scatchard analysis of these data affords complex, nonlinear plots (data not shown). To estimate the binding selectivity of these PTCDIs, a comparison of the change in absorbance at 550 nm for each ligand in the presence of G4-DNA, G4′-DNA, dsDNA, and ssDNA, as in Figure 7, was done (Table 1). Those ligands that demonstrate a large change in the absorbance at 550 nm in the presence of G-quadruplex DNA when compared to the absorbance change in the presence of either dsDNA or ssDNA are deemed to be more selective in their interaction with G-quadruplex DNA than those ligands that demonstrate large changes in the 550 nm absorbance values in the presence of both G-quadruplex DNA and dsDNA or ssDNA.

From the data in Table 1, it can be seen that PIPER and Tel03 are the least selective ligands. The ratios of the $\Delta A_{550\ nm}$ values for G-quadruplex DNA to that for double-stranded DNA for these PTCDIs are 2 and 1.4, respectively. These two ligands are also the least aggregated at pH 7, as evidenced by their relatively strong fluorescence in solution (Table 1). Tel01, Tel04, and Tel10 have low fluorescent emissions correlating to extensive aggregation in solution. These three PTCDIs are also the most selective ligands. The behavior of PTCDI Tel08 is interesting in that it displays only a modest fluorescence in solution and also has a level of selectivity that is intermediate between the extensively aggregated PTCDIs and the nonaggregated PTCDIs; however, the selectivity of Tel08 remains rather low, indicating that extensive PTCDI aggregation is required for a high degree of G-quadruplex DNA binding selectivity.

As further proof of the pH-dependent, aggregate-mediated PTCDI G-quadruplex binding selectivity, absorption spectroscopy experiments were performed under conditions where PIPER was aggregated and Tel01 was not. PIPER is highly aggregated at pH 8.5, as evidenced by a low fluorescence and a strong RLS signal. The absorbance data for PIPER in the presence of G4-DNA and dsDNA collected at pH 8.5 show greatly enhanced selectivity, with a ratio of $\Delta A_{550\ nm}$ for G4-DNA and $\Delta A_{550\ nm}$ for dsDNA of 42 (Table 1). Tel01, which displayed selective binding at pH 7, was assayed at pH 6.4. Under these conditions, Tel01 is not extensively aggregated, as evidenced by a strong fluorescence signal. At this pH, Tel01 displays little selectivity for binding to G-quadruplex DNA; the ratio of $\Delta A_{550\ nm}$ for G4-DNA and $\Delta A_{550\ nm}$ for dsDNA is 1.6 (Table 1).

DISCUSSION

G-quadruplex DNA is a diverse family of higher-order DNA structures that may play a role in telomere maintenance, transcriptional control, chromosome organization, recombination, and other biological processes. These potential roles of G-quadruplex DNA structures have stimulated a search for specific ligands that might serve either as biological probes for these structures or perhaps as therapeutic agents. The search for G-quadruplex DNA binding agents has led to the discovery of a number of different classes of ligands with varying degrees of G-quadruplex DNA selectivity. However, in no case has the origin of the selectivity of a ligand for G-quadruplex DNA versus double-stranded DNA been addressed. We have investigated one class of G-quadruplex DNA ligands, the PTCDIs, and show that for these ligands, G-quadruplex DNA binding selectivity is mediated by ligand self-assembly.

Initial reports of the G-quadruplex DNA binding ability of the PTCDI PIPER demonstrated the ability of this ligand to stack on the terminal G-tetrad faces of G-quadruplex DNA structures, to enhance an intramolecular G-quadruplex-mediated transcription stop site, and to inhibit human telomerase (*35*). Subsequently, PIPER was reported to facilitate the formation of G-quadruplex DNA structure from single-stranded (*37*) and certain double-stranded DNA sequences (*38*). Interestingly, in both gel-shift experiments and NMR titrations involving double-stranded DNA, PIPER demonstrated only slight interactions, indicative of a high degree of selectivity for G-quadruplex DNA over double-stranded DNA (*38*). This selectivity for G-quadruplex DNA binding is reflected in PIPER's ability to selectively inhibit the G-quadruplex DNA unwinding, but not the double-stranded DNA unwinding ability, of the RecQ DNA helicase *Sgs*I (*36*).

By employing absorption spectrophotometric methods, we previously reported that at pH 7 PIPER interacted with both double-stranded DNA as well as G-quadruplex DNA (*14*). In contrast, a related PTCDI, Tel01, demonstrated a much more selective interaction with G-quadruplex DNA at this pH (*14*). Here we show by NMR that there is no obvious structural difference between the complexes formed by PIPER and Tel01 with the G-quadruplex form of d(TAGGGTTA) that could explain the observed differences in binding selectivity between these two compounds. We furthermore demonstrate that PIPER does indeed interact with double-stranded DNA under the conditions of the topoisomerase I assay, and that the result is unwinding of the DNA in a manner analogous to double-stranded DNA intercalation agents.

The PTCDIs are known to undergo aggregation (*56*), and here we demonstrate by a variety of techniques that the

PTCDIs PIPER, Tel01, and related analogues with basic side chains undergo pH-mediated aggregation. The pH at which these PTCDIs aggregate is a function of the basicity of the side chain group. For PTCDIs with more basic side chains (e.g., PIPER, Tel03), aggregation occurs at pH values > 7, whereas for PTCDIs with less basic side chains (e.g., Tel01, Tel04, Tel10), aggregation occurs at neutral pH. This aggregation can be extremely sensitive to small pH changes; pH differences as small as 0.1 unit can have a profound effect on the aggregation state of these PTCDIs. The G-quadruplex DNA binding selectivity of these PTCDIs is directly related to their aggregation state. At neutral pH, the PTCDIs that are aggregated at pH 7 demonstrate enhanced G-quadruplex DNA binding selectivity, and the PTCDIs that are not aggregated at pH 7 display diminished G-quadruplex DNA binding selectivity. Furthermore, by adjusting the pH, the aggregation state of the ligands can be changed. At pH 8.5, PIPER is aggregated and displays enhanced G-quadruplex DNA binding ability relative to that determined at pH 7, where PIPER is not aggregated. Tel01 is not aggregated at pH 6.4, and demonstrates diminished G-quadruplex DNA binding selectivity at this pH compared to that determined at pH 7, where it is aggregated.

The finding of ligand aggregation-mediated G-quadruplex DNA binding selectivity for PIPER and other PTCDI ligands helps to reconcile the conflicting reports of the G-quadruplex DNA binding selectivity of PIPER. Although PIPER does not demonstrate strong interaction with double-stranded DNA during NMR titrations (*38*), the conditions employed, particularly the relative high salt and ligand concentrations, favor aggregation of this ligand. Similarly, assays in which PIPER does not demonstrate significant interaction with double-stranded DNA by gel shift (*37*) or helicase unwinding effects (*36*) were carried out at pH >7, where ligand aggregation is favored. Here we demonstrate that PIPER is selective for G-quadruplex DNA binding under basic conditions where PIPER is aggregated. Thus, despite the modest G-quadruplex DNA binding selectivity of PIPER in the monomeric state, under a variety of assay conditions PIPER is aggregated and does display selective G-quadruplex DNA binding.

A wide variety of small organic molecules are known to undergo aggregation, and this aggregation can lead to nonspecific inhibition of enzymes complicating high-throughput screening methods (*57*). In contrast to this aggregation-mediated promiscuity, the aggregation of PTCDIs leads to increased selectivity in their binding interactions with G-quadruplex DNA targets. The implication of this aggregation-mediated selectivity for other G-quadruplex ligands is not yet known; however, it should be noted that many G-quadruplex DNA ligands contain extended chromophores that may favor ligand aggregation.

The way in which ligand aggregation of the PTCDIs mediates G-quadruplex DNA binding selectivity is not clear. One possibility involves a direct role of the aggregate in G-quadruplex DNA binding. The NMR-based G-quadruplex DNA binding models for both PIPER and Tel01 place the ligands at the 3′ G-tetrad of the DNA, with one face of the PTCDI chromophore stacking over the G-tetrad and the opposite face of the chromophore free, or having only weak associations with the 3′ tail of the G-quadruplex structure. Thus, an aggregated PTCDI with two available chromophore faces at either end of the face-to-face stacked aggregate of (*n*) PTCDI monomers might also interact with the G-quadruplex DNA by this G-tetrad stacking mode. The result of such an interaction would be an intermediate G-quadruplex DNA−PTCDI aggregate complex that could dissociate to afford the G-quadruplex DNA−PTCDI monomer complex and an ($n - 1$) PTCDI aggregate. By this process, direct interaction between the PTCDI aggregate and G-quadruplex DNA would result in deaggregation of the ligand and formation of monomer PTCDI−G-quadruplex DNA complexes. In contrast, the aggregated PTCDI would not be able to interact with double-stranded DNA. Based upon the topoisomerase unwinding results for PIPER, we consider that under conditions where the PTCDIs bind to double-stranded DNA (i.e., in the nonaggregated state) they do so by intercalation. The intercalation of the ligands into double-stranded DNA requires the insertion of the ligand chromophore between DNA base pairs. This process is possible for the monomeric PTCDIs, but not for the aggregated ligands, in which opposite ligand faces are occluded due to the nature of the self-association. Alternatively, assuming that the aggregated PTCDIs exist in equilibrium with a small number of monomeric ligands, the aggregation-mediated G-quadruplex DNA binding selectivity reported here might arise from a competition between monomeric ligand associations with different DNA structures versus self-association. In the case of G-quadruplex DNA, the association of the monomeric PTCDI with the G-quadruplex DNA is more favorable than self-association, whereas in the case of double-stranded DNA, the competition favors the formation of the aggregate. Further work is required in order to define the mechanism by which aggregation leads to selective G-quadruplex DNA binding by these PTCDI ligands.

In conclusion, study of a series of PTCDI bearing basic side chains has demonstrated that these ligands bind to G-quadruplex DNA. Significantly, the selectivity of the G-quadruplex DNA versus double-stranded DNA binding by these PTCDIs is related to the pH-dependent aggregation state of the ligands, such that pH conditions which favor ligand aggregation result in more selective binding interactions with G-quadruplex DNA when compared to nonaggregating pH conditions. The discovery of the aggregation-mediated G-quadruplex DNA binding selectivity exhibited by these compounds may enable their use as tunable biological probes. This work also serves to lay the foundation for improving G-quadruplex selectivity of these PTCDI ligands by rational design of ligands with altered self-assembly proclivity.

ACKNOWLEDGMENT

We acknowledge Steve Sorey for his assistance with NMR experiments and Dr. Miguel Salazar for generous use of the DNA synthesizer.

SUPPORTING INFORMATION AVAILABLE

Chemical shift assignments of the $[d(TAGGGTTA)]_4$−Tel01 complex and ^1H NMR spectra of Tel01, Tel03, Tel04, Tel08, and Tel10. This material is available free of charge via the Internet at http://pubs.acs.org.

REFERENCES

1. Meyne, J., Ratliff, R. L., and Moyzis, R. K. (1989) *Proc. Natl. Acad. Sci. U.S.A. 86*, 7049−7053.

2. Blackburn, E. H. (1994) *Cell 77*, 621−623.
3. Lee, M. S., Gallagher, R. C., Bradley, J., and Blackburn, E. H. (1993) *Cold Spring Harbor Symp. Quant. Biol. 58*, 707−718.
4. Linger, J., and Cech, T. R. (1996) *Proc. Natl. Acad. Sci. U.S.A. 93*, 10712−10717.
5. Kim, N. W., Piatyszek, M. A., Prowse, K. R., Harley, C. B., West, M. D., Ho, P. L. C., Coviello, G. M., Wright, W. E., Weinrich, R. L., and Shay, J. W. (1994) *Science 266*, 2011−2015.
6. O'Reilly, M., Teichmann, S. A., and Rhodes, D. (1999) *Curr. Opin. Struct. Biol. 9*, 58−65.
7. Gilbert, D. E., and Feigon, J. (1999) *Curr. Opin. Struct. Biol. 9*, 305−314.
8. Williamson, J. R. (1994) *Annu. Rev. Biomol. Struct. 23*, 703−730.
9. Kerwin, S. M. (2000) *Curr. Pharm. Des. 6*, 441−471.
10. Simonsson, T. (2001) *Biol. Chem. Hoppe-Seyler 382*, 621−628.
11. Zahler, A. M., Williamson, J. R., Cech, T. R., and Prescott, D. M. (1991) *Nature 350*, 718−720.
12. Fletcher, T. M., Sun, D., Salazar, M., and Hurley, L. H. (1998) *Biochemistry 37*, 5536−5541.
13. Neidle, S., and Read, M. A. (2001) *Biopolymers 56*, 195−208.
14. Kerwin, S. M., Chen, G., Kern, J. T., and Thomas, P. W. (2002) *Bioorg. Med. Chem. Lett. 12*, 447−450.
15. Guo, Q., Lu, M., Marky, L. A., and Kallenbach, N. R. (1992) *Biochemistry 31*, 2451−2455.
16. Kerwin, S. M., Sun, D., Kern, J. T., Rangan, A., and Thomas, P. W. (2001) *Bioorg. Med. Chem. Lett. 11*, 2411−2414.
17. Chen, Q., Kuntz, I. D., and Shafer, R. H. (1996) *Proc. Natl. Acad. Sci. U.S.A. 93*, 2635−2639.
18. Read, M. A., and Neidle, S. (2000) *Biochemistry 39*, 13422−13432.
19. Neidle, S., Harrison, R. J., Reszka, A. P., and Read, M. A. (2000) *Pharmacol. Ther. 85*, 133−139.
20. Han, F. X., Wheelhouse, R. T., and Hurley, L. H. (1999) *J. Am. Chem. Soc. 121*, 3561−3570.
21. Anantha, N., Azam, M., and Sheardy, R. D. (1998) *Biochemistry 37*, 2709−2714.
22. Arthanari, H., Basu, S., Kawano, T. L., and Bolton, P. H. (1998) *Nucleic Acids Res. 26*, 3724−3728.
23. Koeppel, F., Riou, J.-F., Laoul, A., Mailliet, P., Arimondo, P. B., Labit, D., Petitgenet, O., Helene, C., and Mergny, J.-L. (2001) *Nucleic Acids Res. 29*, 1087−1096.
24. David, W. M., Brodbelt, J., Kerwin, S. M., and Thomas, P. W. (2002) *Anal. Chem. 74*, 2029−2033.
25. Duan, W., Rangan, A., Vankayalapati, H., Kim, M.-Y., Zeng, Q., Sun, D., Han, H., Fedoroff, O. Y., Nishioka, D., Rha, S. Y., Izbicka, E., Von Hoff, D. D., and Hurley, L. H. (2001) *Mol. Cancer Ther. 1*, 102−120.
26. Collins, K. (2000) *Curr. Opin. Cell Biol. 12*, 378−383.
27. Mergny, J.-L., Lacroix, L., Teulade-Fichou, M.-P., Hounsou, C., Guittat, L., Hourau, M., Arimondo, P. B., Vigneron, J. P., Lehn, J.-M., Riou, J.-F., Garestier, T., and Helene, C. (2001) *Proc. Natl. Acad. Sci. U.S.A. 98*, 3062−3067.
28. Gowan, S. M., Harrison, J. R., Patterson, L., Valenti, M., Read, M. A., Neidle, S., and Kelland, L. R. (2002) *Mol. Pharmacol. 61*, 1154−1162.
29. Mergny, J.-L., Mailliet, P., Lavell, F., Riou, J.-F., Laoul, A., and Helene, C. (1999) *Anti-Cancer Drug Des. 14*, 327−339.
30. Han, H., and Hurley, L. H. (2000) *Trends Pharmacol. Sci. 21*, 136−142.
31. Perry, P. J., and Jenkins, T. C. (1999) *Exp. Opin. Ther. Pat. 8*, 1567−1586.
32. Mergny, J.-L., and Helene, C. (1998) *Nat. Med. 4*, 1366−1367.
33. Perry, P. J., and Jenkins, T. C. (2001) *Mini-Rev. Med. Chem. 1*, 31−41.
34. Ewing, T. J. A., Makino, S., Skillman, A. G., and Kuntz, I. D. (2001) *J. Comput.-Aided Mol. Des. 15*, 411−428.
35. Federoff, O. Y., Salazar, M., Han, H., Chemeris, V. V., Kerwin, S. M., and Hurley, L. H. (1998) *Biochemistry 37*, 12367−12374.
36. Han, H., Bennett, R. J., and Hurley, L. H. (2000) *Biochemistry 39*, 9311−9316.
37. Han, H., Cliff, C. L., and Hurley, L. H. (1999) *Biochemistry 38*, 6981−6986.
38. Rangan, A., Federoff, O. Y., and Hurley, L. H. (2001) *J. Biol. Chem. 276*, 4640−4646.
39. Liu, Z.-R., and Rill, R. L. (1996) *Anal. Biochem. 236*, 139−145.
40. Kano, K., Fukuda, K., Wakami, H., Nishiyabu, R., and Pasternack, R. F. (2000) *J. Am. Chem. Soc. 122*, 7494−7502.
41. Daffy, L. M., de Silva, A. P., Gunaratne, H. Q. N., Huber, C., Lynch, P. L. M., Werner, T., and Wolfbeis, O. S. (1998) *Chem. Eur. J. 4*, 1810−1815.
42. Pasternack, R. F., Bustamante, C., Collings, P. J., Giannetto, A., and Gibbs, E. J. (1993) *J. Am. Chem Soc. 115*, 5393−5399.
43. Pasternack, R. F., Goldsmith, J. I., Szep, S., and Gibbs, E. J. (1998) *Biophys. J. 75*, 1024−1031.
44. Wang, M., Silva, G. L., and Armitage, B. A. (2000) *J. Am. Chem. Soc. 122*, 9977−9986.
45. Khromov-Borisov, N. V., Indenbom, M. L., and Danilov, A. F. (1980) *Pharm. Chem. J. 14*, 90−93.
46. Plateau, P., and Gueron, M. (1982) *J. Am. Chem. Soc. 104*, 7310−7311.
47. Hare, D. R., Wemmer, D. E., Chou, S.-H., and Drobny, G. (1983) *J. Mol. Biol. 171*, 319−336.
48. Shen, L. L. (2001) *Methods Mol. Biol. 95*, 149−160.
49. Randazzo, A., Galeone, A., and Mayol, L. (2001) *Chem. Commun.*, 1030−1031.
50. Zeng, Q., Kwok, Y., Kerwin, S. M., Mangold, G., and Hurley, L. H. (1998) *J. Med. Chem. 41*, 4273−4278.
51. Shida, T., Ikeda, N., and Sekiguchi, J. (1996) *Nucleosides Nucleotides 151*, 599−605.
52. Pasternack, R. F., and Collings, P. J. (1995) *Science 269*, 935−939.
53. Ford, W. E. (1987) *J. Photochem. 37*, 1889−204.
54. Kasha, M., Rawls, H. R., and Ashraf El-Bayoumi, M. (1965) *Pure Appl. Chem. 11*, 371−392.
55. Rademacher, A., Markle, S., and Langhals, H. C. (1982) *Chem. Ber. 115*, 2927−2934.
56. Wurthner, F., Thalacker, C., Diele, S., and Tschierke, C. (2001) *Chem. Eur. J. 7*, 2245−2253.
57. McGovern, S. L., Caselli, E., Grigorieff, N., and Shoichet, B. K. (2002) *J. Med. Chem. 45*, 1712−1722.

BI0263107